ELSEVIER

Applied Catalysis B: Environmental 27 (2000) 49–63

APPLIED CATALYSIS B: ENVIRONMENTAL

www.elsevier.com/locate/apcatb

Redox behavior of CeO_2–ZrO_2 mixed oxides I. Influence of redox treatments on high surface area catalysts

H. Vidal [a,c], J. Kašpar [a,*], M. Pijolat [b], G. Colon [b,1], S. Bernal [c], A. Cordón [c], V. Perrichon [d], F. Fally [d,2]

[a] *Dipartimento di Scienze Chimiche, Università di Trieste, Via Giorgieri 1, 34127 Trieste, Italy*

[b] *Laboratoire de Procédés des Milieux Granulaires, URA 2021 CNRS, Ecole Nationale Superieure des Mines, 158 Cours Fauriel, 42023 Saint Etienne Cedex-2, France*

[c] *Departamento de Ciencia de los Materiales e Ingeniería Metalúrgica y Química Inorgánica, Universidad de Cádiz, 11510 Puerto Real, Spain*

[d] *Laboratoire d'Application de la Chimie à l'Environnement, UMR 5634, CNRS-Université C.Bernard-Lyon I, 43, Bd. Du 11 Novembre 1918, F. 69622 Villeurbanne Cedex, France*

Received 10 November 1999; received in revised form 13 February 2000; accepted 27 February 2000

Abstract

Redox and textural/structural properties of high surface area ceria–zirconia mixed oxides with composition ranging from 0 to 85 mol% of ZrO_2, have been studied using Raman spectroscopy, X-ray diffraction, textural characterization, magnetic susceptibility measurements, temperature-programmed reduction and oxidation, oxygen storage and buffering capacity measurements. Special attention was given to the effects of aging under redox conditions.

Correlation between chemical composition, textural, structural and redox properties of the oxides is reported. While for pure ceria almost no reducibility occurs below 773 K, mixed oxides, independently of their composition, exhibit an oxygen storage and buffering capacity at low temperature, which remains stable even after several oxidation/reduction cycles. This improvement with respect to CeO_2 is remarkably high in the oxides with high zirconia content and is not affected by worsening of textural properties induced by redox-aging. Phase transformation and/or structural modification are detected as a consequence of the redox treatments, which could be at the origin of such effects.

Keywords: CeO_2–ZrO_2 mixed oxides; Oxygen storage capacity (OSC); CeO_2–ZrO_2 mixed oxides; Temperature-programmed reduction/oxidation (TPR/TPO); Oxygen buffering capacity (OBC); Magnetic susceptibility; Raman spectroscopy; X-ray diffraction

1. Introduction

Ceria–zirconia mixed oxides represent the state-of-art of the so-called oxygen storage capacity (OSC) promoters in automotive exhaust-treatment catalysts [1]. The ability of CeO_2-based promoters to act as an oxygen buffer by releasing/uptaking oxygen through redox processes involving the Ce^{4+}/Ce^{3+} couple,

* Corresponding author. Fax: +39-040-676-3903.
E-mail address: kaspar@univ.trieste.it (J. Kašpar)

[1] On leave from Instituto de Ciencia de Materiales-CSIC, Avda. Americo Vespucio s/n, Isla de la Cartuja, 41092 Sevilla, Spain.

[2] On leave from Facultes Universitaires Notre-Dame de la Paix, Laboratoire LISE, Rue de Bruxelles 61, 5000 Namur, Belgium.

0926-3373/00/$ – see front matter
PII: S0926-3373(00)00138-7

i.e. the OSC, provides a way to increase the efficiency of three-way catalysts (TWCs) by enlarging the air-to-fuel operating window. Improved stability against thermal sintering as well as enhanced redox properties with respect to CeO_2 have been suggested as the main advantages of mixed oxides [2–4].

Despite the large number of investigation on the origin of these improved properties (see for example [1] and references therein), which have been published in the past, except a few studies carried out on highly sintered samples [5,6], a systematic investigation of the influence of textural properties/composition of the mixed oxides on the redox behavior has not been reported so far. A systematic comprehension of the influence of texture and pre-treatments upon the redox properties of the CeO_2–ZrO_2 mixed oxides is necessary, since it has been shown that both these factors affect such properties [7,8]. In the context of the CEZIRENCAT [3] European network project we prepared low and high surface area ceria–zirconia mixed oxides, whose textural/structural characterization was reported recently [9]. The aim of this project is to systematically study CeO_2–ZrO_2 mixed oxides of comparable textural properties but different compositions. The use of well characterized materials should provide a deep insight into the redox properties of these systems, which are of crucial importance for the development of an advanced TWC technology [1].

The results on the redox behavior of high surface area CeO_2–ZrO_2 mixed oxides are reported here. An important point, specifically addressed in this paper, is the investigation of the effects of redox treatments on the chemical/structural properties of these mixed oxides. Emphasis is given on the effects of a deep reduction/mild oxidation redox treatments. Such treatments were shown to favorably affect the reduction behavior of a $Ce_{0.5}Zr_{0.5}O_2$ mixed oxide [7,10–12].

2. Experimental

CEZIRENCAT oxides were synthesized by Rhodia. A detailed characterization is reported in [9]. Hereafter they will be referred to as CZ-XX/YY-HS, where 'HS' indicates that the oxide has a high surface area ($\approx$100 $m^2\,g^{-1}$), and 'XX/YY' indicates the Ce/Zr molar ratio (15/85, 50/50, 68/32, 80/20 and 100/0).

N_2 adsorption/desorption isotherms at 77 K were obtained on a Micromeritics 2100E instrument.

Temperature-programmed reduction (TPR) and oxidation (TPO) studies were carried out in a conventional system equipped with a thermal conductivity detector (TCD). The amount of catalyst used was 50 mg in all cases. After a standard cleaning pre-treatment [13], in O_2 (5%)/Ar at 823 K for 1 h, the samples were slowly cooled down to 473 K; the flow was then switched to Ar (20 ml min^{-1}) and the samples were cooled down to room temperature (RT). TPR was carried out in a flow of 5% H_2/Ar (25 ml min^{-1}, heating rate of 10 K min^{-1}) up to 1273 K. Then the sample was held at this temperature for 30 min. The flow was switched to Ar after 15 min at 1273 K, and the sample was then slowly cooled down to 700 K (or to RT in the case of the TPO experiments). At this point the sample was re-oxidized by pulses of oxygen (0.125 ml) every 75 s. To investigate the effects of redox aging each reducing/oxidizing sequence was performed three times. A sample subjected to such experiments will be hereafter indicated as 'redox cycled'. In selected experiments the reduction was carried out up to 773 or 973 K and held at this temperature for 1 h before the O_2 uptake measurements.

Magnetic susceptibility measurements were carried out with a Faraday microbalance coupled with a high vacuum system. The experimental set up and the procedure for calculation of the magnetic susceptibilities have been described elsewhere [14,15]. The method allows the determination of the content of paramagnetic Ce^{3+} ion. Oxygen buffering capacity (OBC) measurement were employed to determine the ability of mixed oxides to attenuate fast oscillations of oxygen partial pressure. These experiments, whose principles and methodology are described in [16], consisted in injecting 0.25 ml O_2 (5%)/He pulses, every 10 s, in the 60 ml min^{-1} inert gas stream. The O_2 content at the outlet of the reactor was measured with a TC detector. The amount of catalyst used in these experiments was 200 mg.

FT-Raman spectra were obtained on a Perkin–Elmer 2000 FT-Raman spectrometer with a diode-pumped YAG laser and a room temperature super InGaAs detector. The laser power was 100–500 mW.

[3] CEZIRENCAT is a multi-laboratory project in the area of three-way catalysis funded by the European Union. Home page http://www.dsch.univ.trieste.it/cezirencat/index.html.

Powder X-ray diffraction patterns were collected on a Siemens D501 diffractometer (Cu Kα). Indexing of the XRD peaks and calculation of both unit cell parameters and mean crystal size were performed according to criteria described in [9].

3. Results and discussion

3.1. Textural study

As mentioned above characterization of fresh samples have been reported previously [9]. Table 1 reports the effect of redox cycles on the textural properties of the CeO_2–ZrO_2 mixed oxides, obtained from N_2 adsorption isotherms at 77 K. The textural stability of the samples appears relatively low under redox conditions, and significant loss of surface area is already detected after the first redox cycle (Table 1). Previous observation on high surface area CeO_2 showed that reducing conditions strongly favor sintering of these materials [17]. A comparison of the isotherms reported in Fig. 1 shows a significant and progressive modification of the isotherm going from fresh sample to redox cycled ones. This behavior, which is representative of the whole series of oxides, shows that the isotherm shape progressively modifies from type IV to type II after redox cycles [18]. In all cases hysteresis loops are observed, but the porosity is decreasing upon redox treatment.

The change in the isotherm/hysteresis is associated with a shift in the pore size distribution to higher pore diameter as shown in Fig. 2. After consecutive redox cycles, the pore volume decreases significantly, particularly for CZ-80/20-HS and CZ-50/50-HS. On the contrary, the pore size distribution remains almost the same after redox treatment in the case of CZ-15/85-HS and a high surface area is measured. Analysis of the *t*-plots revealed no significant microporosity for any of the samples (results not shown).

3.2. Temperature-programmed reduction, oxygen storage and oxygen buffering experiments

3.2.1. Temperature-programmed reduction

TPR profiles of fresh and redox cycled CZ-XX/YY-HS mixed oxides are reported in Fig. 3. All fresh samples show essentially a single broad reduction feature centered around 850 K. In contrast to CeO_2 sample the well known TPR profile featuring two peaks at 770 and 1100 K (data not shown), which have been, respectively, attributed to the reduction of the surface and in the bulk [19]. The temperatures of the peak maxima/shoulders and the overall oxygen uptakes mea-

Table 1
Textural properties of the CEZIRENCAT oxides

Sample	Number of cycles	S_{BET} ($m^2\,g^{-1}$)	S_t[a] ($m^2\,g^{-1}$)	Cumulative pore volume ($cm^3\,g^{-1}$)	V_{micro} ($cm^3\,g^{-1}$)	Average pore diameter (Å)
CZ 100/0-HS	0	100	94	0.204	0.0020	65
CZ 80/20-HS	0	111	105	0.212	0.0003	40
	1	25	21	0.198	0.0003	220
	3	16	11	0.145	0.0019	260
CZ 68/32-HS	0	100	97	0.259	0.0007	65
	1	63	57	0.239	0.0010	98
	3	28	25	0.200	0.0010	220
CZ 50/50-HS	0	106	99	0.228	0.0018	55
	1	41	36	0.181	0.0016	150
	3	22	19	0.158	0.0011	220
CZ 15/85-HS	0	95	95	0.324	0.0006	95
	1	67	61	0.310	0.0013	125
	3	57	53	0.277	0.0003	120

[a] Surface area detected from *t*-plot.

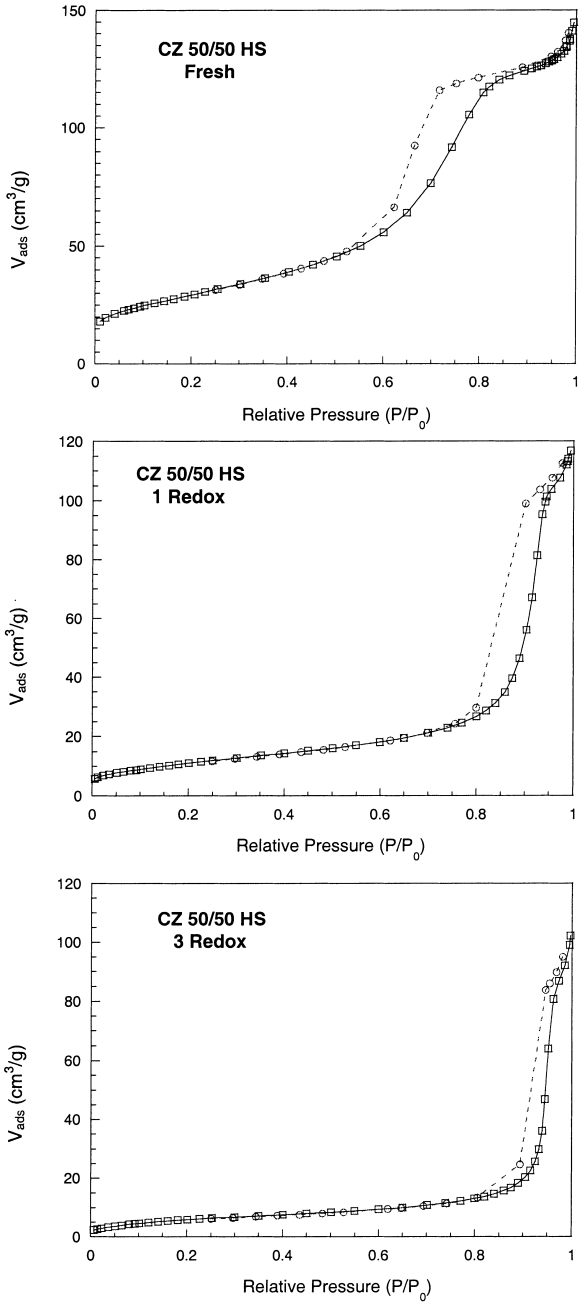

Fig. 1. Effect of redox cycling on the adsorption/desorption isotherms of CZ-50/50-HS.

sured after the TPR experiments (total-OSC) are reported in Table 2.

A perusal of TPR profiles and data in Table 2 reveals a number of interesting aspects. Fresh CeO_2–ZrO_2 samples predominantly show a single reduction feature, albeit some peak tailing or minor peaks are observed above 900 K. This broad H_2 consumption at high temperatures could be associated either with some sample inhomogeneity [20], H_2 adsorption/desorption or some kind of buyoancy effect, i.e. baseline derive due to sample sintering/compacting during the experiment. In the case of CZ-15/85-HS there is an additional reduction feature at moderate temperature (around 660 K).

The temperature of the main peak in the TPR experiments over fresh samples slightly shifts towards lower temperature as the ceria content in the mixed oxides increases (Fig. 4). Consecutive redox-cycling significantly modifies the TPR profiles (Figs. 3 and 4). Consistently with previous reports, all the low temperature redox activity is suppressed after the initial TPR on pure CeO_2 (results not shown), due to the loss of surface area [7]. In contrast, all CeO_2–ZrO_2 samples preserve their redox properties, which are even improved by redox cycling (notice the formation of shoulders at low temperatures for the TPR2 and TPR3 profiles in Fig. 3). The overall picture suggests that reduction in the bulk is improved in mixed oxides compared to pure CeO_2. Furthermore, despite the initial high surface area of the samples, the redox processes occurring at the surface and in the bulk cannot be distinguished under our experimental conditions. As shown in Fig. 3, the most significant change already occurs in the TPR2 experiment and further redox-cycling does not further modify the TPR profile. Effects of redox-cycling strongly depend on the Ce content. Apparently, the formation of the low temperature shoulder/peak is favored by an increase in the Zr content. In fact, in TPR2 and TPR3 profiles of CZ-15/85-HS the main reduction feature becomes the new peak formed around 660 K, which is about 185 K lower than the main TPR peak in the fresh sample. In contrast, the TPR spectra of CZ-80/20-HS are slightly affected by the redox-cycling and the improvement of the reduction at low temperature is hardly visible.

The temperatures of the peak maxima are plotted in Fig. 4 as a function of Ce content. It appears clearly that for equal pre-treatment, the temperature at the maximum of reduction is strongly dependent on the Zr content. Intriguingly, the effect of Zr content reported in Fig. 4 depends on whether fresh or redox-cycled samples are considered. In the case of CeO_2, the

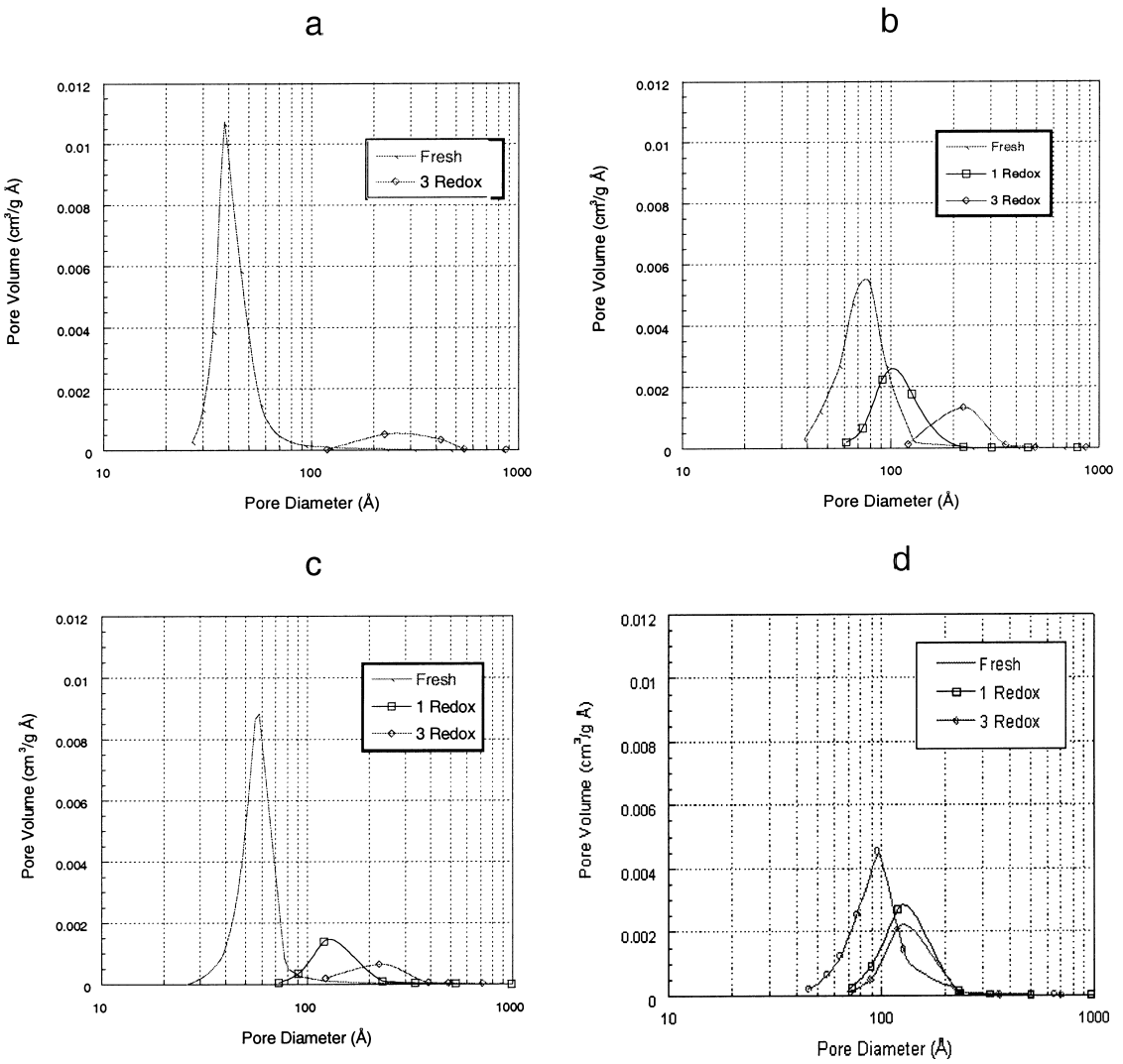

Fig. 2. Effect of redox cycling on the pore size distribution of (a) CZ-80/20-HS; (b) CZ-68/32-HS; (c) CZ-50/50-HS and (d) CZ-15/85-HS.

remarkable deactivation induced by redox cycling is caused by the disappearance of the peak at 770 K — surface reduction — in the TPR profile of the recycled CeO_2. For fresh CeO_2–ZrO_2 mixed oxides samples, an increase of Ce content induces a decrease of reduction temperature, while the opposite behavior is observed in the redox cycled ones. This observation could interpret some contradictory results reported in the literature. It was reported that either high Ce [6] or high Zr [5] contents positively affect the redox activity of CeO_2–ZrO_2 mixed oxides, by decreasing the reduction temperature. In fact, it has been shown that the TPR behavior of these mixed oxides depends on different factors such as pre-treatment conditions,degree of sintering and phase nature [5,7,21]. An important point, however, arises from the present observations: irrespectively of the fine details of the redox pre-treatment, i.e. single or multiple redox-aging, the reduction behavior is strongly modified and improved by the first deep reduction/mild (700 K) oxidation sequence. In contrast, very minor changes are observed in the subsequent redox cycles.

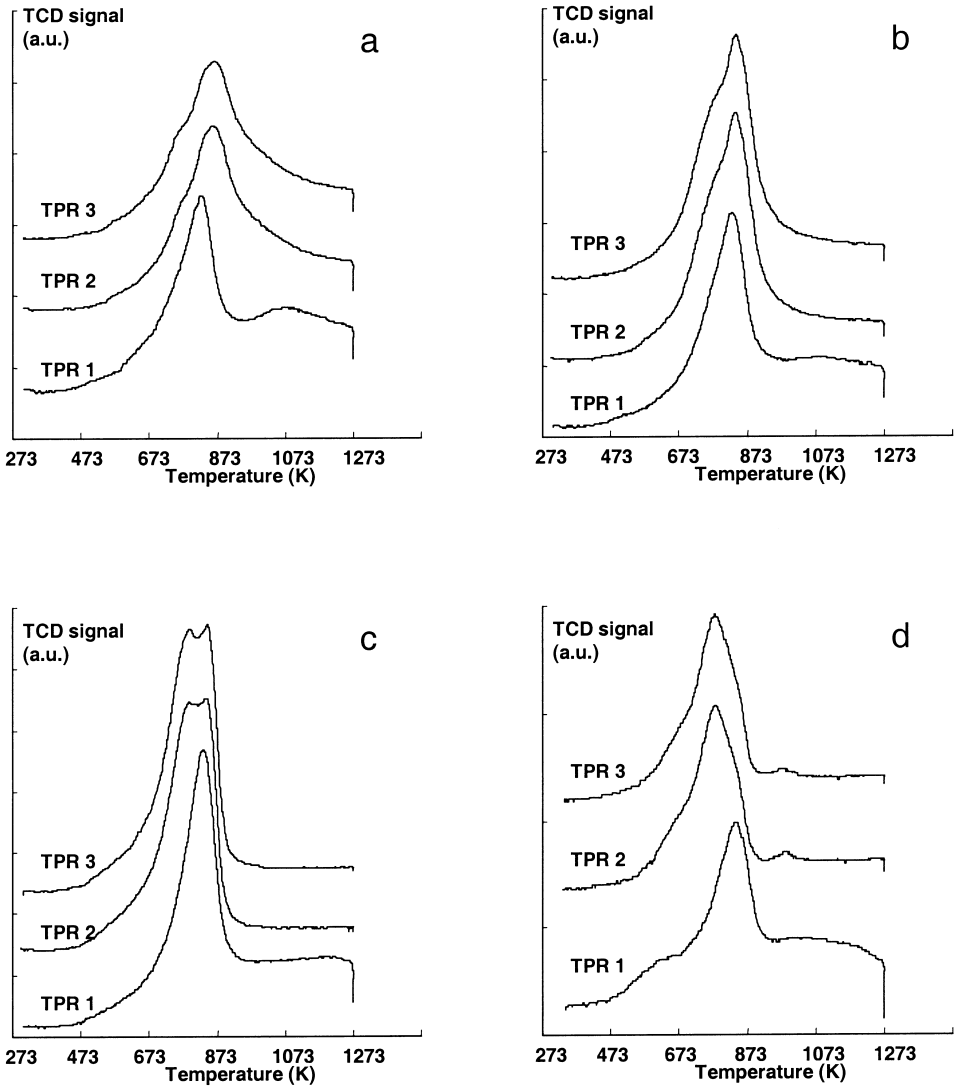

Fig. 3. Effect of redox cycling on the TPR profiles of (a) CZ-80/20-HS; (b) CZ-68/32-HS; (c) CZ-50/50-HS and (d) CZ-15/85-HS.

3.2.2. OSC and TPO measurements

The total-OSC was measured after each TPR experiment by re-oxidizing the samples with pulses of O_2 at 700 K. This procedure, rather than using H_2 consumption, was chosen to avoid artifacts due to surface/bulk impurities and/or H_2 adsorption/desorption phenomena [21]. At 700 K the sample is fully re-oxidized, O_2 adsorption is negligible and, therefore, the O_2 uptake can be taken as the measure of the amount of oxygen vacancies created upon reduction [5].

The obtained values are reported in Table 2. In principle, two types of OSC measurements may be distinguished: dynamic- and total-OSC [19,22]. The latter value, which is reported here, represents the maximum amount of transferable oxygen at a given temperature. As shown by the data reported in Table 2, despite the strong change of textural properties, the total-OSC appears unaffected by the redox cycles, since constant values are observed for all the samples.

Table 2
Temperatures of TPR peak maxima and O_2 uptakes measured at 700 K over the CEZIRENCAT oxides: effects of TPR/oxidation cycles

Sample	Number of cycles	Peak maximum (K)	O_2 uptake (mmol g^{-1})[a]	Ce^{3+} (%)[b]
CZ-100/0-HS	0	790, 1170	0.55	38
	1	1130	0.57	39
	2	1130	0.57	39
CZ-80/20-HS	0	830	0.67	55
	1	790, 865	0.70	57
	2	790, 865	0.69	56
CZ-68/32-HS	0	830	0.72	66
	1	795, 845	0.73	68
	2	795, 845	0.72	67
CZ-50/50-HS	0	835	0.74	87
	1	805, 835	0.73	87
	2	800, 840	0.73	87
CZ-15/85-HS	0	655, 845	0.26	92
	1	670, 790	0.26	91
	2	660, 790	0.27	93

[a] Standard deviation ± 0.01 mmol g^{-1}.
[b] Estimated from the O_2 uptake, assuming a full re-oxidation of the reduced sample.

Fig. 5a shows that the degree of reduction, expressed as percentage of Ce^{3+}, strongly increases with the zirconium content. Thus, the chemical composition does have an influence on the reducibility of Ce^{4+} sites. However, as shown in Fig. 5b, the O_2 uptake after reduction at 973 and 1273 K is almost the same for samples 80/20, 68/32 and 50/50 indicating that a constant amount of oxygen vacancies is created in these three samples upon reduction. This indicates that the differences in structures of fresh samples, e.g. changes from cubic to tetragonal (t′ and t″) phase decreasing Zr content from 80 to 50 mol% [9], are not responsible for the reduced state of these samples after reduction at high temperature. At a reduction temperature of 773 K the situation becomes different. The increase of the Ce content from 15 to 80 mol% results in a decrease of Ce^{3+} content for the whole range of the oxides. However, due to the high Ce content, the OSC is highest in the CZ-80/20-HS sample. Recently, it was observed that the rate-limiting step of the reduction of CeO_2–ZrO_2 mixed oxides using H_2 as reductant changes with the reduction temperature [23]. This could account for the different dependency of OSC upon ZrO_2 content with the temperature of reduction, reported in Fig. 5b.

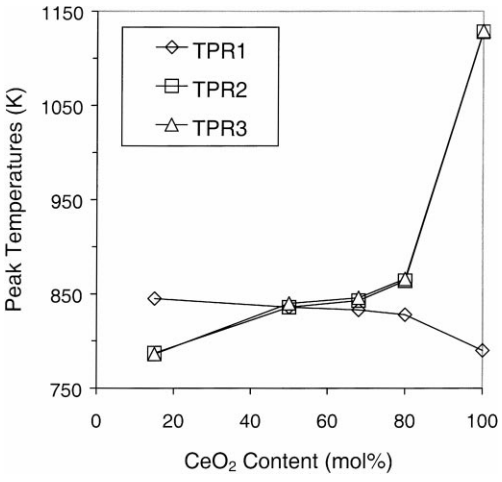

Fig. 4. Temperatures of the maximum reduction rate in the TPR profiles as function of the composition.

The extent of reduction of the CZ-15/85-HS sample appears to be related to the limited amount of Ce^{4+} available for reduction, besides the differences in structural properties. As much as 95% of Ce^{4+} is indeed reduced during the TPR experiment.

The re-oxidation process was investigated by pulsing O_2 over the catalysts at 700 K and by TPO experiments. The results are reported in Figs. 6 and 7. At 700 K re-oxidation easily proceeds into the bulk in all the samples investigated (Fig. 6), even if some subtle

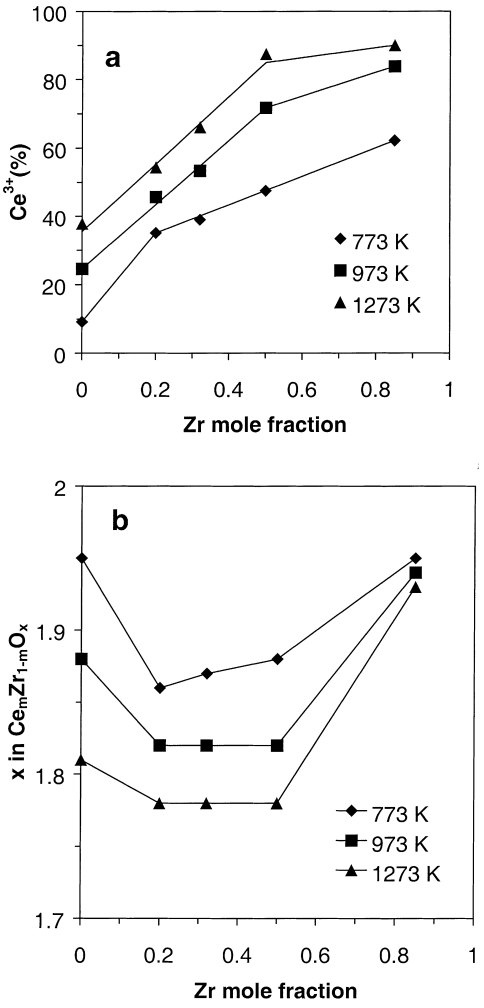

Fig. 5. Cerium reducibility as function of the zirconium content (a) and amount of oxygen vacancies expressed as x in $Ce_mZr_{1-m}O_x$; (b) estimated from the O_2 uptake at 700 K. Reduction temperature as indicated in the figure. The lines are only an eye-guide.

differences exist. In fact, the cumulative oxygen uptake linearly increases up to 80–100% of re-oxidation in CZ-100/0-HS, CZ-50/50-HS and CZ-15/85-HS samples, while in other cases (CZ-68/32-HS and CZ-80/20-HS) deviation from linearity occurs when about 40% of Ce^{3+} is re-oxidized. A linear increase of the cumulative O_2 uptake is an indication that all the O_2 pulsed over the reduced catalysts is consumed, indicating that the re-oxidation at 700 K is fast and easy at any degree of reduction. In contrast, the behavior observed for the CZ-68/32-HS and CZ-80/20-HS

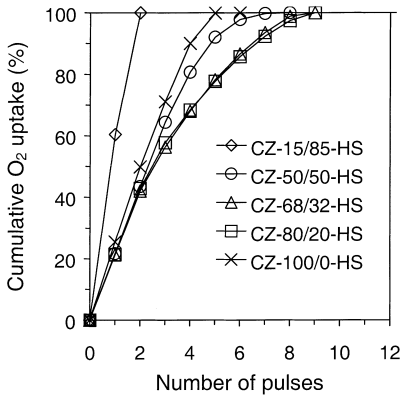

Fig. 6. Cumulative O_2 uptake obtained in the re-oxidation at 700 K of CZ mixed oxides reduced at 1273 K: (×) CZ-100/0-HS; (□) CZ-80/20-HS; (△) CZ-68/32-HS; (○) CZ-50/50-HS and (◇) CZ-15/85-HS.

samples suggests that in this case re-oxidation/O_2 uptake is relatively slow compared to the residence time of the O_2 pulse over the catalyst ($\leq$0.04 s). Therefore, it appears that the chemical composition affects the rate of the re-oxidation process as well. Noticeably, the kinetics of re-oxidation of each sample remains almost invariant with the redox cycling (results not shown).

Excluding CeO_2, which is known to be easily re-oxidized [24], the re-oxidation of the mixed oxides is easier with high zirconium content. This trend is the opposite of what is observed in the TPR profiles of fresh samples (Fig. 4), but consistent with redox cycled samples. Since the oxygen uptake was measured on samples reduced at 1273 K, this behavior should be preferably related to redox cycled ones. Accordingly, it appears that the promptness of a sample to release or store oxygen is best correlated with the TPR behavior of the redox-cycled samples.

The TPO profiles reported in Fig. 7 indicates that most of the re-oxidation takes place at RT. Only about 10–25% of the total-OSC corresponds to re-oxidation occurring around 373 K. No further O_2 adsorption was detected above 700 K (data not shown). Once again the oxidation behavior of the CZ-68/32-HS and CZ-80/20-HS sample somewhat differs from that of the other compositions as detected by the strong tailing of the re-oxidation peak detected at RT. This is in agreement with a slow kinetic for the re-oxidation of these samples.

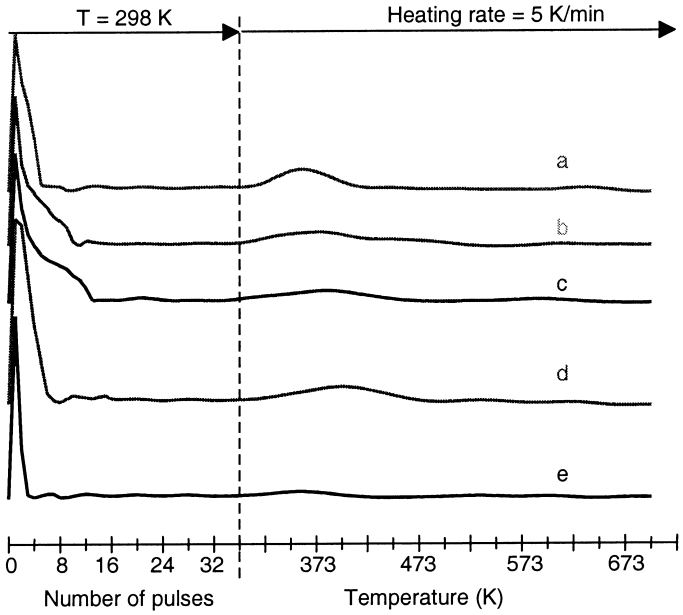

Fig. 7. TPO profiles of CZ mixed oxides reduced at 1273 K: (a) CZ-100/0-HS; (b) CZ-80/20-HS; (c) CZ-68/32-HS; (d) CZ-50/50-HS and (e) CZ-15/85-HS.

3.2.3. OBC experiments

Table 3 summarizes the results obtained from the OBC experiments. A typical OBC experiment is depicted in Fig. 8 for the CZ-68/32-HS sample.

Table 3
Oxygen buffering capacity (%) of the CEZIRENCAT oxides as function of temperature: effects of redox cycling

Sample	Number of cycles	673 K	923 K	1173 K
CZ-100/0-HS	0	0	0	<1
	1	0	0	<1
	3	0	0	<1
CZ-80/20-HS	0	2	28	78
	1	5	34	80
	3	5	23	76
CZ-68/32-HS	0	1	34	82
	1	6	36	83
	3	3	36	85
CZ-50/50-HS	0	5	36	83
	1	3	44	85
	3	4	46	89
CZ-15/85-HS	0	6	29	72
	1	3	36	85
	3	6	33	

As shown by the data reported in Table 3, the ability to attenuate fast partial oxygen pressure oscillations of both fresh and redox-cycled samples increases with temperature, from 673 to 1173 K. The only exception is CeO_2, which showed only negligible activity. Except at 673 K, CZ-68/32-HS and CZ-50/50-HS systems are more efficient OBC systems. A remarkable observation is that the OBC is unaffected by redox cycling despite the strong decrease of the surface area (compare Section 3.1). Generally speaking under dynamic condition, redox processes should involve mostly the surface [19]. A constant OBC or even its improvement upon redox cycling, is a strong indication that under our experimental conditions bulk/subsurface oxygen atoms are readily available for redox processes. Notice that the enhancement of reducibility with redox cycling observed in the TPR experiments is confirmed by the OBC technique. This suggests that the redox behavior as detected by the TPR profiles is relevant to the redox processes occurring under dynamic conditions. The increase of OBC with redox cycling is noticeably high in the case of CZ-15/85-HS. It is consistent with its TPR behavior and seems to be correlated with the

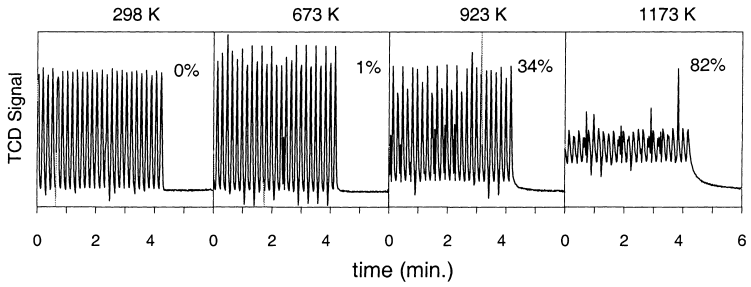

Fig. 8. OBC experiments carried on the fresh CZ-68/32-HS sample at different temperatures.

changes in the structure underwent by this sample upon redox cycling (see below).

3.3. Magnetic susceptibility measurements

Magnetic susceptibility measurements were carried out in a magnetic balance under flowing H_2 (5%)/He. Reduction (5% H_2/He, 1 h) was carried out by increasing the reduction temperatures from 298 to 973 K. Magnetic susceptibility measurements were performed after cooling to RT under the same hydrogen mixture. Reduction percentages, calculated on a $[Ce^{3+}]/[Ce^{3+}+Ce^{4+}]$ basis, are presented versus temperature in Fig. 9. The redox properties of mixed oxides are improved compared to CeO_2: the reduction begins at lower temperature and higher reducibility is observed at $T \leq 973$ K. In addition, no clear distinction can be made between the reduction of surface and bulk ions, in agreement with the TPR results. In contrast, a quasi plateau in the reducibility curve of CeO_2 was found between 770 and 870 K [25]. This is consistent with a significantly higher contribution of bulk oxygen species of solid solutions compared to CeO_2.

The total-OSC obtained from the Ce^{3+} percentage measured in these experiments lead to the same conclusion (Fig. 10). A clear improvement of the OSC is evidenced for CZ- 80/20, 68/32 and 50/50 mixed oxides compared to CeO_2. The values obtained for these mixed oxides are remarkably similar. Concerning the CZ-15/85 HS oxide, although the cerium ions were

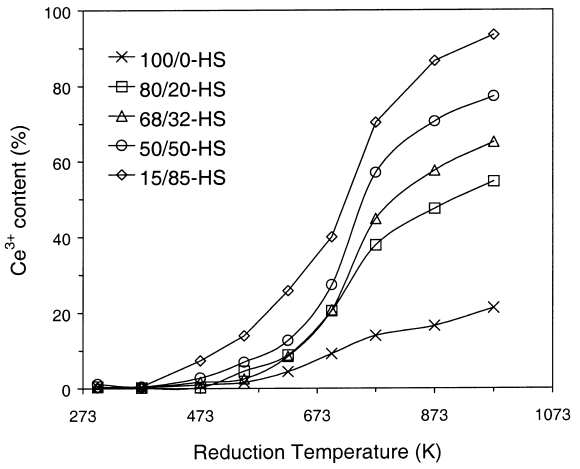

Fig. 9. Reduction percentages of the $Ce_{1-x}Zr_xO_2$ solid solutions obtained from the magnetic susceptibility as a function of the reduction temperature (1 h at each temperature).

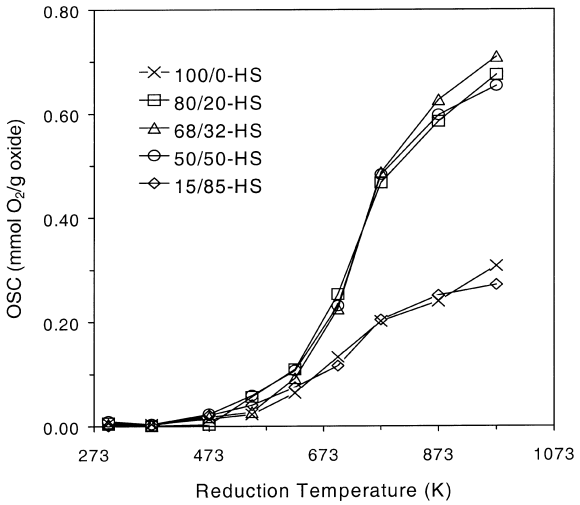

Fig. 10. Oxygen loss (mmol of O_2 per gram of oxide) estimated from the Ce^{3+} percentages for the $Ce_{1-x}Zr_xO_2$ solid solutions calculated from magnetic susceptibility as a function of the reduction temperature (1 h at each temperature).

Table 4
Ce^{3+} percentages (%) obtained after reduction at 973 K under H_2 (5%)/He, after oxidation under oxygen (40 Torr) of the reduced samples, at 298 K and after oxidation at 823 K

x In $Ce_{1-x}Zr_xO_2$	Ce^{3+} percentages[a] Treatment conditions		
	After reduction at 973 K under H_2 (5%)/He	At 298 K, under 40 Torr O_2	After heating at 823 K under O_2 (40 Torr)
0.20	54.6	1.3	0.8
0.32	65.1	1.5	0.7
0.50	77.2	2.2	1.7
0.85	93.4	0.1	0.0

[a] Ce^{3+} percentages estimated from the magnetic susceptibility measurements.

the most easily reduced in the series of mixed oxides (Fig. 9), its OSC is close to that of ceria due to the limited cerium content. After reduction at 973 K the highest OSC is obtained for $Ce_{0.68}Zr_{0.32}O_2$ (0.71 mmol O_2 per gram of oxide). There is a very good agreement with the OSC values estimated from the pulse experiments (Table 2), which indicates that only Ce^{4+} reduction is involved.

RT re-oxidation of the samples reduced at 973 K was carried out in the magnetic balance by introducing small doses of pure oxygen with a leak valve. Table 4 gives the residual Ce^{3+} percentages after re-oxidation of the samples under 40 Torr of O_2 at 298 K and after heating at 823 K.

The re-oxidation is fast and nearly completed at room temperature, the residual Ce^{3+} content after oxidation at 298 K being lower than 2.2%. After the treatment at 823 K, there is only a small change in this percentage, confirming that the initial oxidation state of cerium in the solid solution is almost restored at RT. The absence of a total re-oxidation observed at RT in the TPO experiment is due to a kinetic control of the re-oxidation in these experiments.

Finally, it should be underlined that a good agreement is obtained between the reduction extents calculated from the magnetic susceptibility and the weight changes during oxygen adsorption. That also indicates that the oxygen vacancies formed during the reduction of the solid solutions are associated with the cerium ions.

3.4. Structural characterization

As shown in Sections 3.2 and 3.3, the reduction of mixed oxides and hence dynamic and total-OSC imply processes occurring both at the surface and in the bulk. In order to get insight to which extent the structural properties may be related to this kind of behavior, both fresh and redox cycled catalysts have been characterized by powder XRD and Raman spectroscopy.

3.4.1. FT Raman spectroscopy

Fig. 11 reports Raman spectra of fresh and redox cycled samples. The attribution of the spectral features has been previously discussed for fresh samples [9]. Only some relevant features are reported here. For Ce content higher then 50 mol%, spectra are dominated by a strong band at 472–478 cm^{-1}. This band is attributed to the F_{2g} vibration of the fluorite type lattice. The appearance of weak bands around 300 and 130 cm^{-1} has been attributed to tetragonal displacement of the oxygen atoms from their ideal fluorite lattice positions leading to phase t″ or t′ [26]. The spectrum of the sample CZ-15/85-HS reveals the presence of small amounts (about 5 mol%) of a *m*-ZrO_2 non-incorporated into the solid solution during the synthesis. For a assignation of the bands we refer the reader to [9,27].

As a general trend, except for CZ-80/20-HS and CeO_2 (data not reported), redox cycling induces noticeable modifications of the Raman spectra. In the case of CZ-80/20-HS (Fig. 11, trace a), the F_{2g} band is slightly displaced to higher frequency. Typically, the insertion of Zr into the CeO_2 lattice shifts the F_{2g} mode to somewhat higher frequencies compared to CeO_2 (465 cm^{-1}) due to cell contraction. Loss of symmetry of the band at 479 cm^{-1} with formation of a shoulder at about 465 cm^{-1} is found in the case of the CZ-68/32-HS. Some CeO_2 segregation cannot be excluded as the origin of this shoulder.

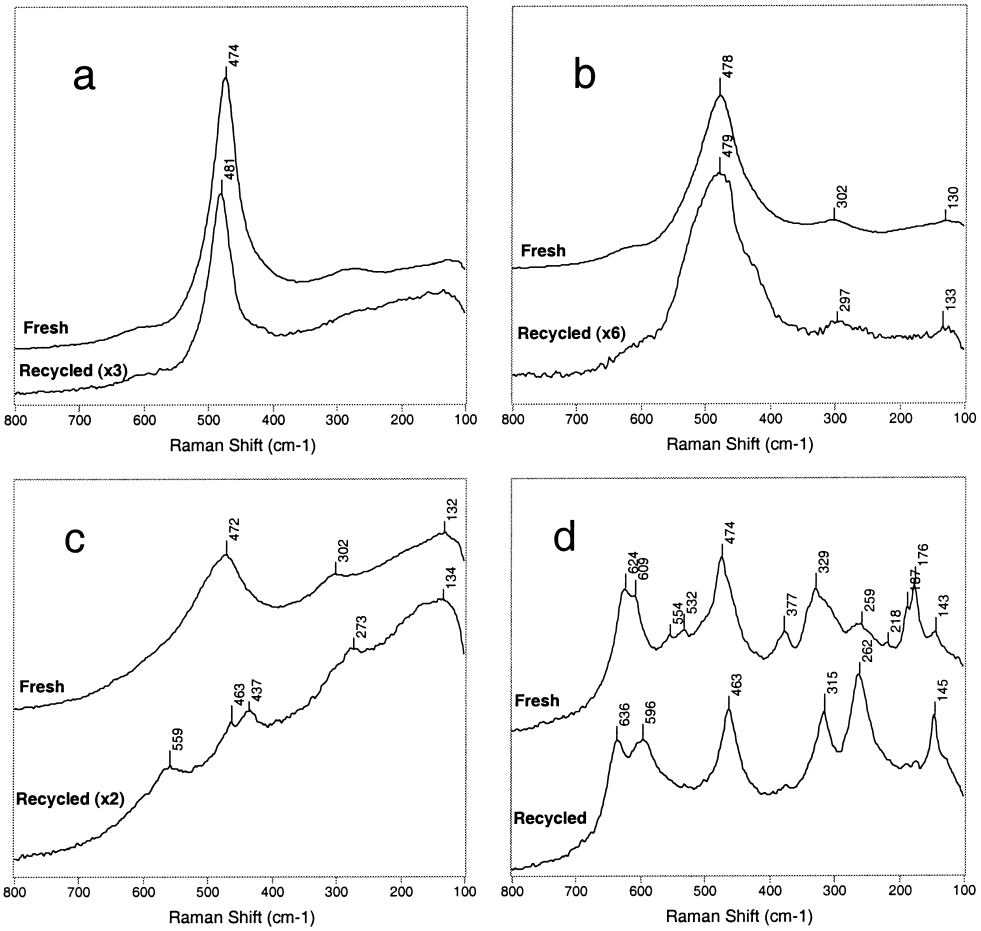

Fig. 11. Raman spectra of fresh and redox cycled (a) CZ-80/20-HS, (b) CZ-68/32-HS, (c) CZ-50/50-HS and (d) CZ-15/85-HS. (Spectra multiplied by the specified factor).

The more striking effects of redox cycling are observed on CZ-50/50-HS and CZ-15/85-HS. In the Raman spectrum of CZ-50/50-HS the band at 472 cm^{-1} disappears and new bands at 437, 463 and 559 cm^{-1} are observed. The band at 463 cm^{-1} can tentatively be attributed either to traces of CeO_2 or to a shift of the F_{2g} band. The band at 302 cm^{-1} shifts to 273 cm^{-1}. This indicates that the original symmetry (t′ or t″ is lost upon redox cycling and new phase(s) are formed. It is also important to note that the intensity of the Raman spectra of recycled samples is far smaller than that of fresh ones. Even though the intensity depends on several factors including grain size and morphology, it should be reminded that sintering of CeO_2 was shown to sharpen and increase the intensity of the F_{2g} band [28]. It is conceivable that sintering of the samples under redox conditions leads to a perturbation of the local symmetry of the M–O bond, which breaks the symmetry selection rules [29].

The strong changes of the Raman spectrum of CZ-15/85-HS induced by redox cycling (Fig. 11d) can be related to the disappearance of the monoclinic phase, originally present in the sample as an impurity, to form a tetragonal solid solution (*t* phase).

3.4.2. X-ray diffraction

Fig. 12 compares the (1 1 1) peak of some of the redox cycled samples. The (1 1 1) peak is progressively displaced to larger angles as the Zr content increases

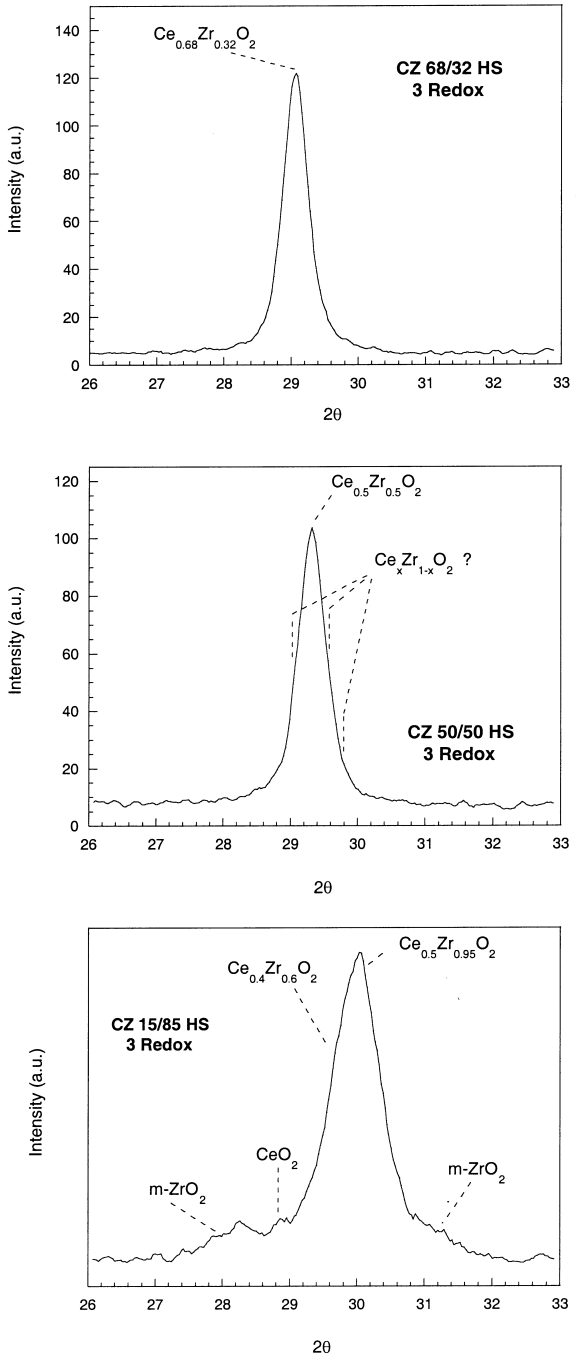

Fig. 12. X-ray diffraction patterns of some CEZIRENCAT oxides after three redox cycles.

from 20 to 50 mol%. This is due to a contraction of lattice cell parameter.

After three redox cycles (Fig. 12), CZ-68/32-HS consists of an almost pure single phase, indicating that even if some small segregation could occur, no substantial change of the XRD pattern occurred. This is not the case for CZ-50/50-HS where some phase transformations are suspected. In fact, the broad (1 1 1) peak cannot account for the presence of a single phase. The presence of minor diffraction peaks (<5%) in this sample can be noticed. Furthermore, the XRD pattern of the redox cycled CZ-15/85-HS sample reveals the presence of new minor phases (<5%). These new phases can be attributed to the presence of two solid solutions: $Ce_{0.4}Zr_{0.6}O_2$ and $Ce_{0.05}Zr_{0.95}O_2$. In addition, the presence of CeO_2, already detected by Raman spectroscopy, cannot be excluded. However, it is worth noting a small peak corresponding to *m*-ZrO_2, which was not observed in the Raman spectra.

The correlation of the above results with the redox behavior is not straightforward. We have to take into account that the situation of the sample in each redox cycle is different, in terms of surface area, crystallite size and composition. We also have to consider that an oxidative treatment could lead to phase segregation in CZ-68/32 and 50/50 as it has been established from thermal stability studies in oxidative conditions [30]. On the other hand, some of our unpublished results of the thermal stability in H_2 atmosphere indicate that segregation is not observed under such conditions, except for CZ-15/85-HS. The investigation of the effects of reducing/oxidizing treatments on the structural properties of CeO_2–ZrO_2 mixed oxides is still in progress, but it appears clearly that the transformations depend on the pre-treatment. However, the overall behavior of the samples through redox cycles indicates that the first redox treatment significantly modifies the structure and the properties of the oxides. The observed structural modifications indicate that the adopted redox cycling procedure acts as an effect of a reducing atmosphere rather than an oxidizing one.

In conclusion, the X-ray study of CEZIRENCAT oxides submitted to redox cycles leads to observations that are in good agreement with the characterization performed by Raman spectroscopy. As discussed above, it is clear that structural modifications take place, the kind of modification being dependent

on the composition. Phase separations, however, appear to be rather limited because of the prevalently reducing nature of our treatments.

4. Conclusions

The present study shows that the unusual redox behavior, e.g. the promotion of reducibility by redox cycling, appears as a general property of high surface area CeO_2–ZrO_2 mixed oxides. The degree of promotion depends on Zr content: High Zr contents favor low temperature reduction of the redox cycled samples. The study of the re-oxidation process leads to results, which are consistent with those derived from TPR experiments. O_2 uptake kinetics, both at 700 K and as a function of temperature (TPO), depend on the composition of the mixed oxide, the re-oxidation of CZ-15/85-HS being the fastest one, however, they are unaffected by the redox cycling.

Magnetic susceptibility measurements confirm that reduction/oxidation processes occur at expenses of the Ce^{4+}/Ce^{3+} redox couple and that no clear distinction can be made between surface and bulk reduction in the mixed oxides.

Finally, structural characterization of redox cycled samples revealed that the structure of redox-cycled mixed oxides changes with the composition and treatment. At a high Ce content, e.g. CZ-80/20-HS, only negligible modifications of the lattice are detected. More significant structural changes are observed at the intermediate composition where significant distortions of the oxygen sublattice are detected. It appears reasonable that such structural changes have some relevance to the OSC property, which in fact depends on the composition and pre-treatment of the CeO_2–ZrO_2 mixed oxide.

Generally speaking, the addition of Zr to ceria in the range 20–50% mole fraction leads to high OSC, which, at high temperatures, is independent of the oxide composition. This is due to the fact that the amount of the oxygen vacancies created upon high temperature reduction treatments is almost constant, leading to an increase of the amount of reduced Ce^{4+} with Zr content. At high Zr content, the redox processes occur promptly, however, the OSC is limited by the small amount of Ce present.

Acknowledgements

Financial support from the TMR Program of the European Commission (Contract FMRX-CT-96-0060) is acknowledged. H. Vidal, G. Colon and F. Fally acknowledge their fellowships from the TMR Program. The authors also thank Dr. R.T. Baker from Depto. de Ciencia de los Materiales e Ingeniería Metalúrgica y Química Inorgánica for preparing the recycled samples that have been used for XRD and textural studies.

References

[1] J. Kaspar, P. Fornasiero, M. Graziani, Catal. Today 50 (1999) 285.
[2] L.L. Murrell, S.J. Tauster, D.R. Anderson, in: A. Crucg (Ed.), Catalysis and Automotive Pollution Control II, Elsevier, Amsterdam, 1991, pp. 275–289.
[3] T. Murota, T. Hasegawa, S. Aozasa, H. Matsui, M. Motoyama, J. Alloys Comp. 193 (1993) 298.
[4] G. Ranga Rao, J. Kaspar, R. Di Monte, S. Meriani, M. Graziani, Catal. Lett. 24 (1994) 107.
[5] P. Fornasiero, R. Di Monte, G. Ranga Rao, J. Kaspar, S. Meriani, A. Trovarelli, M. Graziani, J. Catal. 151 (1995) 168.
[6] A. Trovarelli, F. Zamar, J. Llorca, C. de Leitenburg, G. Dolcetti, J.T. Kiss, J. Catal. 169 (1997) 490.
[7] P. Fornasiero, G. Balducci, R. Di Monte, J. Kaspar, V. Sergo, G. Gubitosa, A. Ferrero, M. Graziani, J. Catal. 164 (1996) 173.
[8] R.T. Baker, S. Bernal, G. Blanco, A.M. Cordon, J.M. Pintado, J.M. Rodriguez-Izquierdo, F. Fally, V. Perrichon, Chem. Commun. (1999) 149.
[9] G. Colon, M. Pijolat, F. Valdivieso, H. Vidal, J. Kaspar, E. Finocchio, M. Daturi, C. Binet, J.C. Lavalley, R.T. Baker, S. Bernal, J. Chem. Soc., Faraday Trans. 94 (1998) 3717.
[10] G. Balducci, P. Fornasiero, R. Di Monte, J. Kaspar, S. Meriani, M. Graziani, Catal. Lett. 33 (1995) 193.
[11] S. Otsuka-Yao, H. Morikawa, N. Izu, K. Okuda, J. Jpn. Inst. Metals 59 (1996) 1237.
[12] S. Otsuka-Yao-Matsuo, T. Omata, N. Izu, H. Kishimoto, J. Solid. State Chem. 138 (1998) 47.
[13] M. Daturi, C. Binet, J.C. Lavalley, H. Vidal, J. Kaspar, M. Graziani, G. Blanchard, J. Chim. Phys. 95 (1998) 2048.
[14] J.P. Candy, V. Perrichon, J. Catal. 89 (1984) 93.
[15] A. Laachir, V. Perrichon, A. Badri, J. Lamotte, E. Catherine, J.C. Lavalley, J. El Fallah, L. Hilaire, F. Le Normand, E. Quemere, N.S. Sauvion, O. Touret, J. Chem. Soc., Faraday Trans. 87 (1991) 1601.
[16] S. Bernal, G. Blanco, M.A. Cauqui, P. Corchado, J.M. Pintado, J.M. Rodriguez-Izquierdo, Chem. Commun. (1997) 1545.
[17] V. Perrichon, A. Laachir, S. Abouarnadasse, O. Touret, G. Blanchard, Appl. Catal. A.: Gen. 129 (1995) 69.

[18] S.J. Gregg, K.S.W. Sing, Adsorption, Surface Area and Porosity, 2nd Edition, Academic Press, New York, 1982.
[19] H.C. Yao, Y.F. Yu Yao, J. Catal. 86 (1984) 254.
[20] P. Vidmar, P. Fornasiero, J. Kaspar, G. Gubitosa, M. Graziani, J. Catal. 171 (1997) 160.
[21] F.M.Z. Zotin, L. Tournayan, J. Varloud, V. Perrichon, R. Frety, Appl. Catal. A.: Gen. 98 (1993) 99.
[22] A. Trovarelli, Catal. Rev. -Sci. Eng. 38 (1996) 439.
[23] P. Fornasiero, J. Kaspar, M. Graziani, Appl. Catal. B: Environ. 22 (1999) L11.
[24] C. Padeste, N.W. Cant, D.L. Trimm, Catal. Lett. 18 (1993) 305.
[25] V. Perrichon, A. Laachir, G. Bergeret, R. Frety, L. Tournayan, O. Touret, J. Chem. Soc., Faraday Trans. 90 (1994) 773.
[26] M. Yashima, H. Arashi, M. Kakihana, M. Yoshimura, J. Am. Ceram. Soc. 77 (1994) 1067.
[27] V.G. Keramidas, W.B. White, J. Am. Ceram. Soc. 57 (1974) 22.
[28] G.W. Graham, W.H. Weber, C.R. Peters, R.K. Usmen, J. Catal. 130 (1991) 310.
[29] P. Fornasiero, E. Fonda, R. Di Monte, G. Vlaic, J. Kaspar, M. Graziani, J. Catal. 187 (1999) 177.
[30] G. Colon, F. Valdivieso, M. Pijolat, R.T. Baker, J.J. Calvino, S. Bernal, Catal. Today 50 (1999) 271.